Design of a 1 t/h Biomass Chain Boiler and Its Fuel Adaptability Analysis

Fu Chengguo[1], Feng Yipeng[1], Tian Yishui[2,*], Liang Mingchao[1] and Zhang Zhengchuan[3]

[1] *School of Mechanical and Electrical Engineering, Henan Institute of Science and Technology, Xinxiang 453003, China*
[2] *Key Laboratory of Energy Resource Utilization from Agricultural Residue of Ministry of Agriculture and Rural Affairs, Chinese Academy of Agricultural Engineering Planning & Design, Beijing 100125, China*
[3] *Engineering Technology Faculty, Sumy National Agrarian University, Sumy 40021, Ukraine*

___

Abstract

The arch is an important component of a biomass boiler. Initial arch design of most boilers is generally gained through manual computation, thus resulting in uncertain reasonability of flue gas flow. Moreover, biomass fuels in the market have instable characteristics, which influence the utilization of biomass energies considerably. To address the problems concerning reasonable flue gas flow caused by the collaborative design of arch and air staging and the combustion adaptability of fuels, a cold modeling experiment of a 1 t/h biomass boiler under different staged air distribution ratios when the rear arch coverage varies was conducted using Fluent software in this study after thermal performance computation and initial structural design of grate and furnace. Furthermore, a boiler performance test based on main fuels and a combustion adaptation test of auxiliary fuels were also performed. The experiments show that the best flue gas flow in the furnace is achieved when the rear arch coverage is 60% and the primary–secondary air distribution ratio is 4:6. The mean boiler efficiency and the mean boiler heat output are 81.26% and 715.76 kW/h by using *Pinus koraiensis* pellets, wood–straw mixed pellets, and cotton straw briquettes as main fuels; and the tested pollutant emissions are in compliance with the limits of the national standard. The results of the combustion adaptation test reveal that the excessive particle size, the high ash content and the relatively low calorific value of biomass molded fuels are all against the combustion of biomass boilers. Fuel upgrading based on washing process and other methods is suggested. This study can provide references to the performance optimization of traditional small-scale biomass chain heating boilers.

Keywords: Biomass molded fuel, Boiler, Arch, Fuel adaptability

___

1. Introduction

Biomass boiler, which is fueled with agricultural and forest residues, is an important device to construct a clean distributed heating system in areas with severe energy shortage [1-4]. The global output of straw resources is approximately 7 billion t/a [5]. Field combustion of straw resources will cause serious particulate pollution [6] and deterioration of soil fertility [7]. Biomass molded fuel (BMF) can replace fossil fuel, and it can be used on large scales for its characteristics of high density, convenient storage and transportation, easy ignition, and good combustion [2,4,8]. It not only can realize waste recycling but also can decrease emissions of greenhouse gases given its carbon-neutral properties [9]. BMF boiler is an important way to realize recycling of agricultural and forest residues [8,11]. A good boiler structural design determines the reasonability of flue gas flow in the furnace, and it is an important means to increase combustion efficiency and decrease pollutant emission [12-14].

Boilers that use biomass energy can be divided into coal–biomass cofiring and biomass boilers. Sangpil [15] investigated 26 power plants in the United States and found that the mixing ratio of biomass (mainly torrefied wood or shells) was 3.7 % –7.2 % when the cost variation was controlled within ±10%. Family boilers were mainly fueled with wood materials. Pawlak-Kruczek [16] tested the

combustion performance of torrefied palm shells in a coal-fired boiler and determined low pollutant emission and stable combustion performance. However, Niu [17] found that the torrefied cost was considerably high, and torrefied palm shells were difficult to be applied on large scales. Biomass is generally prepared into BMF directly. Although wood materials have stable performance, the physical and chemical properties of straw are significantly influenced by its categories, fertilization, and other regional factors. Moreover, the N content in straw fuel is generally high and is unstable in different batches [18]. Compared with coal, biomass has a relatively higher volatile content, and it stores more than 2/3 quantity of heat. Therefore, biomass boiler has to be redesigned to prevent reduction of combustion efficiency and performance. Chu [19] found by studying a reciprocating grate boiler that rear arch coverage length was the primary influencing factor of combustion, followed by front arch coverage length and the inclination angle of the rear arch. Front arch height could influence the combustion performance in the reciprocating grate boiler the least. These study conclusions provide some references to chain boilers. Just [20], Liu [21], and other researchers [22-26] mainly adopted gas–solid separated combustion and air staging in the development of a biomass boiler, which effectively prolonged the residence time of smoke and increased combustion efficiency. NO_x emission was also decreased significantly with the introduction of a low-nitrogen combustion technology. Nevertheless, most associated studies have only adjusted operator parameters in boiler optimization, but few have changed the furnace structure.

The conventional momentum synthesis technique [27] is a furnace arch design based on experiment. Theoretically, it assures " α -shaped" flue gas flow in the primary combustion zone to make smoke and air mix thoroughly and promote complete combustion in the secondary combustion space. Zheng [28] cited such information in the design of a 4 t/h BMF boiler, but he did not verify the flue gas flow. Chse [29] investigated the influence of secondary air injection angle on combustion and concluded that given a fixed excess air ratio, the secondary air injection angle influenced CO concentration slightly, but it would influence flame shape and might cause production of thermal NO_x . Song [30] analyzed the influences of inner and outer secondary air distribution on combustion. However, such an exquisite secondary air distribution is mainly for boilers in power stations and is rare in ordinary heating boilers. Luo [31] proposed a "zigzag-shaped" improved scheme for the traditional arch of an open furnace, but this scheme is essentially for staged combustion and air staging. Chen [32,33] constructed a fuel layer combustion numerical model and simulated the combustion in the entire chain boiler. Although the model achieved high simulation accuracy, the chain boiler technology was relatively mature, and the overall simulation was inconsiderably necessary.

The aforementioned research results mainly focus on fuel layer combustion modeling and overall simulation of pollutant emission. Few studies have been conducted on the arch design of boilers. Most boiler computations are still accomplished using the traditional computational method. The computation cost and time consumption during overall combustion simulation of a designed boiler are considerable,

and the furnace and arch are difficult to modify even though the boiler structure is optimized. Therefore, furnace and arch shall be designed with air staging in the design process of a biomass boiler. Moreover, boiler test shall include the adaptation of multiple fuels.

In this study, the design of a 1 t/h biomass chain boiler with atmospheric pressure was regarded as an example. The influencing laws of rear arch coverage and staged air distribution on the flow path of flue gas were analyzed through CFD simulation to determine relatively better arch design and staged air distribution after arch and furnace structures were gained using the traditional computational method. BMF stability greatly fluctuates in the market due to the extensive sources of biomass. Hence, a performance test of boiler based on main fuel was conducted to verify the designs of furnace and arch. A combustion adaptation test based on auxiliary fuels was also performed, and relevant improvement measures were proposed.

2. Materials and Methods

2.1 General methods
The biomass boiler has the form of a chain grate stoker. Grate and furnace are designed on the basis of industrial analysis, element analysis, and combustion characteristics of the fed Pinus koraiensis pellets (Table 1) [34]. A cold modeling experiment in the furnace is conducted, and the relevant furnace structure is determined. Lastly, a performance test of the boiler is performed, and fuel adaptability is analyzed.

Table 1. Industrial and element analyses of BMF

| BMF source	BMF category	Industrial analysis (%)			Element analysis (%)					Low heat value (LHV)
		V_{daf}	M_{ar}	A_{ar}	C_{ar}	O_{ar}	H_{ar}	N_{ar}	S_{ar}	$Q_{net,ar}$ (kJ/kg)
Fed fuel	P. koraiensis	70.34	7.08	7.75	43.81	34.2	5.66	0.97	0.53	16491
Main fuels in the market	P. koraiensis	86.35	8.80	0.52	47.55	37.45	5.80	0	0.01	17730
	Wood–straw	65.40	10.00	8.29	43.67	32.56	4.90	0.54	0.10	15860
	Cotton straw	66.12	3.32	16.24	46.22	27.67	4.84	1.25	0.47	16103
Independently made by enterprises	Rice hull– duck manure	54.40	8.34	24.31	35.04	40.25	4.88	1.20	0.32	11114
	Corn–wheat	64.40	6.34	16.16	42.15	38.25	5.38	0.48	0.06	12760

The boiler efficiency test is accomplished using the drainage method in accordance with GB/T 10180-2014. The atmospheric pollutant test method is based on the following standards: GB/T 16157-1996, GB/T 5468-91, HJ/T 398-2007, HJ 693-2014, and HJ/T 57-2017.

The instruments and equipment in this study include a microcomputer smoke parallel sampling machine (Wuhan Tianhong Environmental Protection Industry Co., Ltd., TH-880F), a smoke analyzer (Testo 335), an electronic scale (BSA, 124S), and a cold-atom Hg absorption tester (ChangZhou Jintan Hengfeng Instrument Manufacturing Co., Ltd., NCG-1).

2.2 Boiler Structure
The structure of the biomass boiler is shown in Fig. 1. Biomass fuels are burned in the grate. The generated high-temperature smoke runs through the outlet between front and rear arches, flows to the smoke–dust separation chamber behind the furnace, turns 180° and flows to the gas pass of " 八 " shape on the two sides of the furnace and the front smoke chamber in front of the shell, and enters into the spirally corrugated tube. The exhaust gas from the boiler is guided to the dust extraction apparatus through the rear

smoke chamber and then enters into the chimney through an induced draft fan. In the rear smoke–dust separation chamber of the furnace, dusts fall at the back of the rear arch by inertia and then into the ash pit through holes. Air is sent by a blower to the air compartment below the grate.
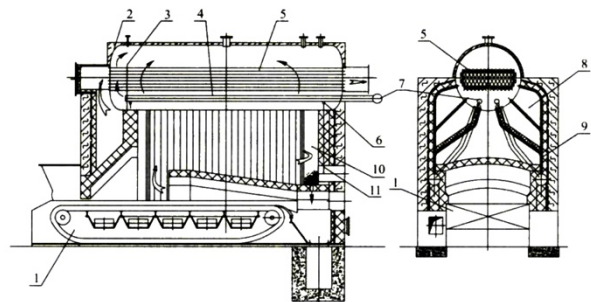
Fig. 1 Structure of a water–fire tube boiler [35]
1-grate; 2-arch tube plate; 3-return water guide housing; 4-return water distribution pipe; 5-spirally corrugated tube; 6-injection pipe; 7-return pipe; 8-gas pass of " 八 " shape; 9-water-cooled wall; 10-smoke–dust separation chamber; 11-downcomer.

2.3 Parametric calculation of boiler
2.3.1 Characteristics of combustion products

$$
\begin{cases}
\alpha_{py}=\alpha_{lc}^{"}=\alpha_{lj}+\Delta\alpha \\
V_k^0 = 0.0889(C_{ar}+0.375S_{ar})+0.265H_{ar}-0.0333O_{ar} \\
V_k = \dfrac{(\alpha_{lc}^{"}+\alpha_{lj})}{2}V_k^0 \\
V_y^0 = V_{RO_2}+V_N^0+V_{H_2O}^0 \\
\quad = 0.01866\times C_{ar}+0.7S_{ar}+0.79\times V_k^0 \\
\quad\quad +0.008\times N_{ar}+0.111H_{ar}+0.0124M_{ar}+0.0161V_k^0 \\
V_y = V_y^0 + 1.016(\alpha_{py}-1)V_k^0
\end{cases}
\quad (1)
$$

where α_{py} is the excess air ratio at the furnace outlet. V_k^0 and V_k are the theoretical air and actual air (m^3/kg) needed for the combustion of 1 kg of biomass completely, respectively. V_y^0 is the theoretical flue gas (m^3/kg) that is generated via the combustion of 1 kg of biomass completely, which includes the volumes of theoretical CO_2, SO_2, N_2, and water vapor. V_y is the actual smoke volume (m^3/kg) that is higher than V_y^0 caused by excess air ratio. Specific calculation results are shown in Table 2.

Table. 2. Calculation results of the characteristics of combustion products

Theoretical air V_k^0 $\left(m^3/kg\right)$	Excess air ratio at the furnace out α_{py}	Theoretical flue gas V_y^0 $\left(m^3/kg\right)$	Actual air V_k $\left(m^3/kg\right)$	Actual flue gas V_y $\left(m^3/kg\right)$
4.273	1.6	4.989	6.20	7.160

2.3.2 Combustion characteristics

The excess air ratio at the furnace outlet is calculated using the following equation:

$$\alpha_{py}=\alpha_{lc}^{"}=\alpha_{lj}+\Delta\alpha \quad (2)$$

The heat loss due to exhaust gas smoke is calculated as follows:

$$q_2 = \frac{(I_{py}-\alpha_{py}I_{lk}^0)(100-q_4)}{Q_r} \quad (3)$$

With main considerations of RO_2, N_2, and H_2O in smoke, I_{py} is the enthalpy of the exhaust gas temperature at 180 °C, which is 2003.81 kJ/kg g. I_{lk}^0 is the enthalpy under cold air at 20 °C, which is 134.8 kJ/kg. These parameters are integrated into Eq. (3), and q_2 is calculated as 10.59%.

The heat loss due to sensible heat in slag is calculated as:

$$q_6 = \frac{a_{lz}(ct)_{lz}A_{ar}}{Q_{net.ar}} \quad (4)$$

where the ash loss is $a_{lz}=1-a_{f,a}$. The flue dust proportion ($a_{f,a}$) is determined as 0.2, and the enthalpy of slag ($(ct)_{lz}$) at 600 °C is 560 kJ/kg.

The heat output of the boiler (Q_1) is calculated using the following equation:

$$Q_1 = 10^3[D(h_{bq}-h_{gs})+D_{pw}(h_{bs}-h_{gs})] \quad (5)$$

where softened water is adopted in the water cycle, and the blowdown flow (D_{pw}) is 0.03 t/h . From the enthalpy tables, the enthalpies of saturated steam (h_{bq}), saturated water (h_{bs}), and feed water (h_{gs}) are 2787.6, 826.1, and 85.4 kJ/kg, respectively. Therefore, the following equation is generated:

$$
\begin{cases}
B = \dfrac{Q_1}{Q_{net.ar}\times\eta} \\
\eta_2=100-\sum q_i \\
\varphi = 1-\dfrac{q_5}{\eta+q_5}
\end{cases}
\quad (6)
$$

where B is the fuel consumption (kg/h), η_2 is the antibalance efficiency (%), i=2–6, and φ is the heat retention coefficient. Relevant main calculation results are listed in Table 3.

Table 3. Basic parameters of heat balance

Heat loss due to exhaust gas $q_2(\%)$	Heat loss due to sensible heat in slag $q_6(\%)$	Heat output $Q_1(\ kJ/h)$	Fuel consumption $B(kg/h)$	Heat retention coefficient φ
10.59	0.21	2724421	197.57	0.976

2.3.3 Indexes of furnace, arch, and grate

2.3.3.1 Furnace indexes

The furnace volume heat release rate (q_V)is 306 kW/m^3. Therefore, the effective furnace volume (V_L, excluding the

fuel and slag layers) and furnace height (H_{lg}) on the grate surface and the space enclosed by both ends of the grate and the vertical plane of the slag back plate can be calculated as follows:

$$\begin{cases} V = \dfrac{BQ_{net,ar}}{3600 \times q_V} \\ H_{lg} = \dfrac{V_L}{A} \end{cases} \tag{7}$$

2.3.3.2 Grate indexes

Scale-type chain grate is applied to assure the relatively low rate of coal leakage. Meanwhile, a roll with side walls is applied at the end of the grate to solve the grate deviation. The entire grate is set horizontally due to the high volatile content of biomass to achieve full mixing of air in the furnace. The heat release rate (q_R) of the grate is 390 kW/m^2 . Then,

$$\begin{cases} A = \dfrac{BQ_{net,ar}}{3600 \times q_R} \\ R_{tf} = B\dfrac{V_k}{3600 \times W_k} \\ f_{tf} = 100\dfrac{R_{tf}}{L_P \times B_P} \end{cases} \tag{8}$$

where R_{tf} is the sectional area of grate ventilation (m^2). f_{tf} is the percentage of air space. $Q_{net,ar}$ is the net LHV as received basis (kJ/kg). B is the fuel amount entered into the boiler per unit time (kg/h). The flow rate of air through the grate (W_k) is set to 2 m/s. A is the effective area of grate (m^2), and it is calculated as 2.32 m^2 after the data in Table 2 and Table 3 are integrated into Eq. (8). The effective width of the grate (B_P) is chosen as 800 mm . Therefore, the effective length of the grate (L_P) is 2900 mm .

2.3.3.3 Arch indexes

The arch is to promote the mixing of gases in the furnace and thereby makes fuels ignited in time. In this study, the conventional arch design method is applied first. The arch structure, which is made of perlite refractory materials, is shown in Fig. 2. The expected arch is determined using the momentum synthesis method [25] to assure flue gas of convolutional " α -shaped" airflow line type below the arch. This condition can increase the heat and mass transfer between smoke and air, prolong the residence time of flue gas, promote complete combustion of fuels, and increase burn-off rate and boiler efficiency.
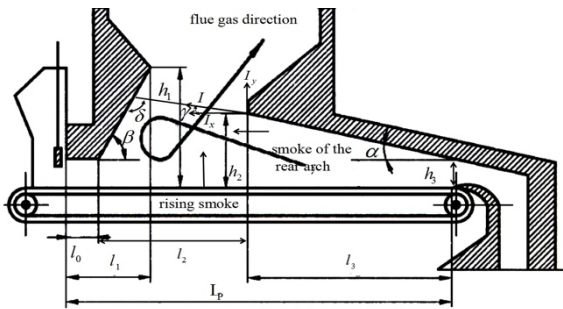

Fig. 2. " α -shaped" flow line-type arch of the chain grate stoker [27]
L_P——length of the grate; l_0——horizontal length of the front arch inlet; l_1——length of the grate under front arch coverage; l_2——

effective length of the front grate; l_3——length of the grate under rear arch coverage; h_1——height of the front arch; h_2——height of the rear arch; h_3——height of the rear arch outlet; α——inclination angle of the rear arch; β——inclination angle of the front arch; γ——momentum synthesis angle; δ——angle between synthesized momentum and the front arch.

The effective heat release (Q_l) of the furnace is calculated using the following equation:

$$Q_l = \frac{Q_{net,ar}(100 - q_3 - q_4 - q_6)}{(100 - q_4)} + \Delta\alpha I_{lk}^0 \tag{9}$$

where I_{lk}^0 is the theoretical enthalpy of input cold air at 20 °C, which is 202.2 kJ/kg . When $\alpha_{lc}^"$ and Q_l are combined, the theoretical combustion temperature (t_{ll}) is 1292 °C in accordance with the enthalpy temperature table. The exhaust gas temperature ($t_l^"$) at the furnace outlet is set to 900 °C . On this basis, the corresponding flue gas temperature at the furnace throat (t_h , °C) and the average smoke temperature (t_y , °C) are calculated as follows:

$$\begin{cases} t_h = 0.5(t_{ll} + t_l^") \\ t_y = 0.5(t_h + t_{ll}) \end{cases} \tag{10}$$

The momentum synthesis angle (γ) can be calculated using the following equations:

$$\begin{cases} V_{y1} = kV_y B_j(t_y + 273)/273 \\ V_{y2} = (1-k)V_y B_j(t_y + 273)/273 \\ W_{y1} = V_{y1}/h_2 B_p \\ W_{y2} = V_{y2}/l_2 B_p \\ I_l = V_{y1}\rho_y W_{y1} \\ I_2 = V_{y2}\rho_y W_{y2} \\ \rho_y = 273\rho_y^0/(t_y + 273) \\ \rho_y^0 = M\rho_k^0 \\ \gamma = \tan((I_1\sin\alpha + I_2)/I_1\cos\alpha) \\ B_j = B \times \dfrac{100 - q_4}{100 \times 3600} \end{cases} \tag{11}$$

where V_{y1} and V_{y2} refer to the flow of smoke at the outlet section of rear arch and the flow of rising smoke (m^3/s), respectively. W_{y1} and W_{y2} are the flow rate of smoke at the outlet section of rear arch and the flow of rising smoke (m/s), respectively. l_2 is the effective length of the front grate, which is 0.82 m in this study. I_l is the momentum of smoke at the rear arch and the rising smoke (N). ρ_k^0 is the air density under standard state (kg/m^3). ρ_y^0 is the smoke density under standard state (kg/m^3). ρ_y is the actual smoke density (kg/m^3). M is the conversion coefficient. B_j is the calculated fuel consumption

(kg/s).The inclination angle of the rear arch is generally 8°–12°, and it is chosen as 10° in this study. On the basis of the calculation, γ is 25.59° , and δ is determined as 113.41° , which meets the determined principle of being larger than 110°. Theoretically, the " α -shaped" flow line can be formed. The results are shown in Table 4.

When the boiler capacity is smaller than or equal to 4 t/h , the height of the rear arch outlet h_2 (m) is calculated as

$$h_2 = \frac{a_2' B_J V_y}{3600 B_P (\omega_g)_{ref}} \frac{\vartheta_g + 273}{273} + h_{co} \qquad (12)$$

where h_{co} is the thickness of the fuel layer, and it is generally 0.1 m. ϑ_g is the average smoke temperature in the rear arch zone, and it is generally 1250 °C (calculated on the basis of coals). a_2' is the rear arch coverage, and it is generally approximately 50 % –65 % to assure complete combustion below the rear arch. In this study, a_2' is set to 55 % , 60 % , and 65 % in the calculation, and the corresponding length of rear arch coverage (a_2) is chosen as 1595, 1740, and 1885 mm , respectively. $(\omega_g)_{ref}$ is the reference smoke velocity at the rear arch outlet, and the recommended reference value of $(\omega_g)_{ref}$ is 4.5–6.5 m/s . It is set to the minimum of 4.5 m/s in this study in consideration of the high volatility of BMF. If the result of Eq. (12) is smaller than 550 mm, then h_2 is 550 mm . The practical calculated result is 465.36 mm ; hence, the determined h_2 is 550 mm in this study. Other important parameters are listed in Table 4.

Table 4. Basic parameters of furnace and grate

Items	Values
Sectional area of grate ventilation $R_t (\text{m}^2)$	0.17
Percentage of air space $f_{tf} (\%)$	7.91
Effective furnace volume $V_L (\text{m}^3)$	2.96
Furnace height $H_{1g} (\text{m})$	1.38
Draft loss in the grate and fuel layer $\Delta H_m (\text{ Pa})$	459.38
Heat retention coefficient φ	0.976
Radiation heating surface $H_f (\text{ m}^2)$	3.26
Active furnace area $F_l (\text{ m}^2)$	8.60
Furnace coverage area $F (\text{ m}^2)$	10.75
Furnace volume $V_l (\text{m}^3)$	3.52
Horizontal length of the inlet end of the front arch $l_0 (\text{ mm})$	340
Front arch height $h_1 (\text{ mm})$	943
Inclination angle of the front arch $\beta (°)$	50.13
Covered grate length of the front arch excluding the inlet length $a_1 (\text{mm})$	618.38
Rear arch height $h_2 (\text{mm})$	550
Inclination angle of the rear arch $\alpha (°)$	10
Height from the rear arch to the grate end $h_3 (\text{mm})$	243.24

2.4 Determination of arch structure and air staging

2.4.1 Requirements on the settings of arch and air staging

Rational designs of front and rear arches and reasonable primary and secondary air distributions can assure the expected flow direction of flue gas and strengthen the full mixing of smoke and air. This condition can increase the combustion efficiency of boilers and decrease pollutant emissions [36]. When the furnace temperature is lower than 1000 °C, it is mainly the fuel-type NO_x reaction mechanism in NO_x emission [37]. In the primary combustion chamber, primary air is supplied from the grate bottom, biomass is dried and pyrolyzed in the grate, and fixed carbon is burned. CO, H_2, $C_x H_y$ $H_2 O$, and N_2 are the main components of flammable gas. Among them, NH_3 , HCN , and NO are beneficial to denitration. The temperature on the grate surface is low due to the insufficient primary air supply for complete combustion, thus inhibiting the slagging phenomenon.

In the upper position of the arch, secondary air is supplied by another blower through opposite blowing between the front and rear arches, which increases the disturbance. The jets are in the front arch (horizontal inclination angle= 12°) and the rear arch (in consistent direction). The secondary air is mixed with volatile components from biomass pyrolysis in the secondary combustion chamber. Later, the mixture is burned to decrease pollutants caused by imperfect combustion. This phenomenon can improve the mixing between flue gases and secondary air, thus increasing the combustion temperature and lowering the overall excess air ratio. Therefore, the pollutant emission caused by imperfect combustion can be decreased.

2.4.2 Cold modeling experiment of furnace

The secondary air flow rates from the nozzles are supposed to be consistent. In this study, a cold modeling experiment of airflow in the entire furnace under different air distribution ratios and rear arch coverages (55 % , 60 % , and 65 %) is conducted using Ansys 13.0-Fluent in accordance with the actual air volume in Table 2. Basic hypotheses are made, as shown as follows:

(1) Particles develop no deformation in the combustion, and the fuel layer is applicable to the porous model. The bulk density of pellets is 600 kg / m^3 , and the height and porosity of the fuel layer are 10 cm and 0.65, respectively.

(2) BMF is fed from the inlet on the left of the grate, and certain air leakage exists. Uniform primary air supply exists from the grate bottom, and the injection speed and air volume at the secondary air outlet are equal.

(3) The air temperature is 20 °C , and settings of primary and secondary air inputs are gained in accordance with the actual flue gas and staged air distribution ratio. These parameters are calculated in Subsection 2.3.

(4) The relative pressures at the material inlet and furnace outlet are set to 0 Pa and −150 Pa respectively.

With reference to the literature [38], 3D simulation of air flow in the furnace space is performed. Calculations are implemented using the standard k-ε model, second-order upward format, and SIMPLE algorithm. A rectangular grid in the fuel layer, triangular (Pave) and quadrilateral (Submap) grids on the furnace surface, and tetrahedral grid (TGrid) in the body are adopted. After grid independence verification, a
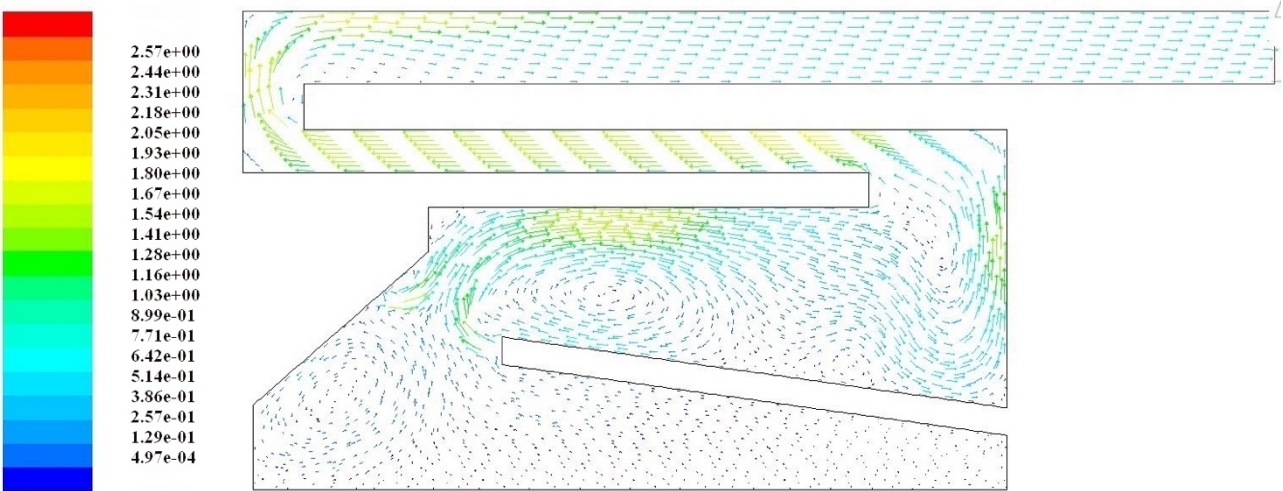
total of 749,506 grids are yielded when the rear arch coverage is 60 %. Fig. 3 shows the results of the relatively enhanced simulation clouds of air staging are gained when the rear arch coverage is 55 %, 60 %, and 65 %.
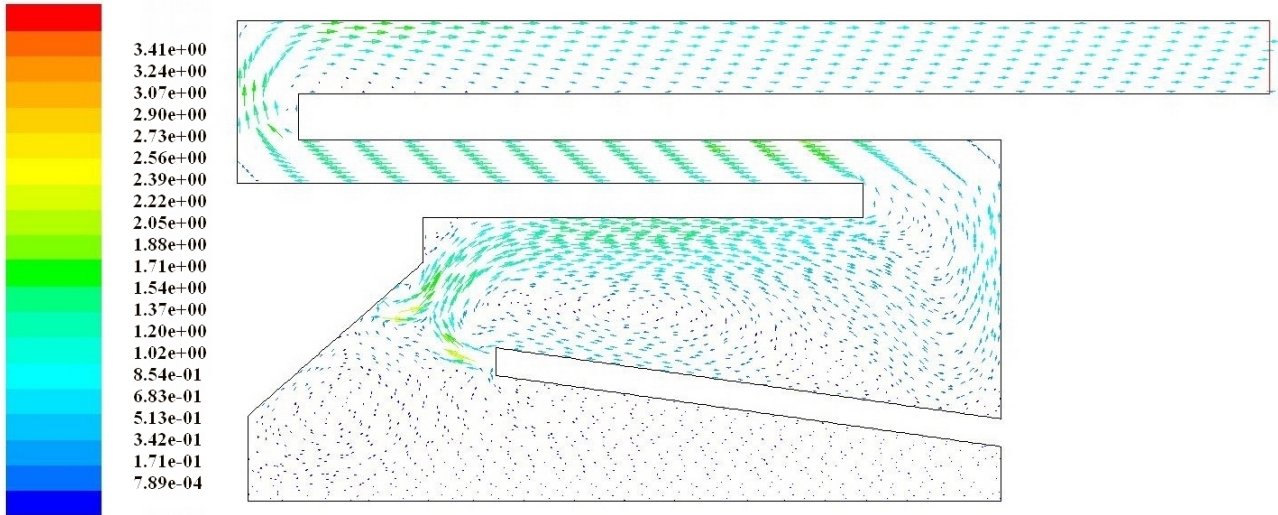

Velocity vectors colored by velocity magnitude (m/s)
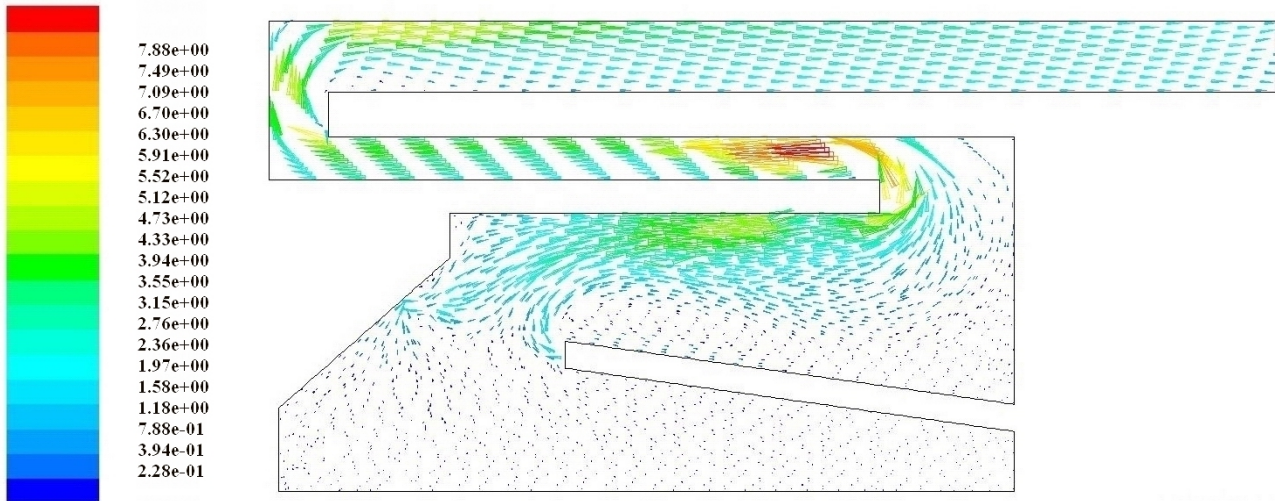
(a) The rear arch coverage is 55 %, and the staged air distribution ratio is 4:6.

Velocity vectors colored by velocity magnitude (m/s)

(b) The rear arch coverage is 60 %, and the staged air distribution ratio is 3:7.
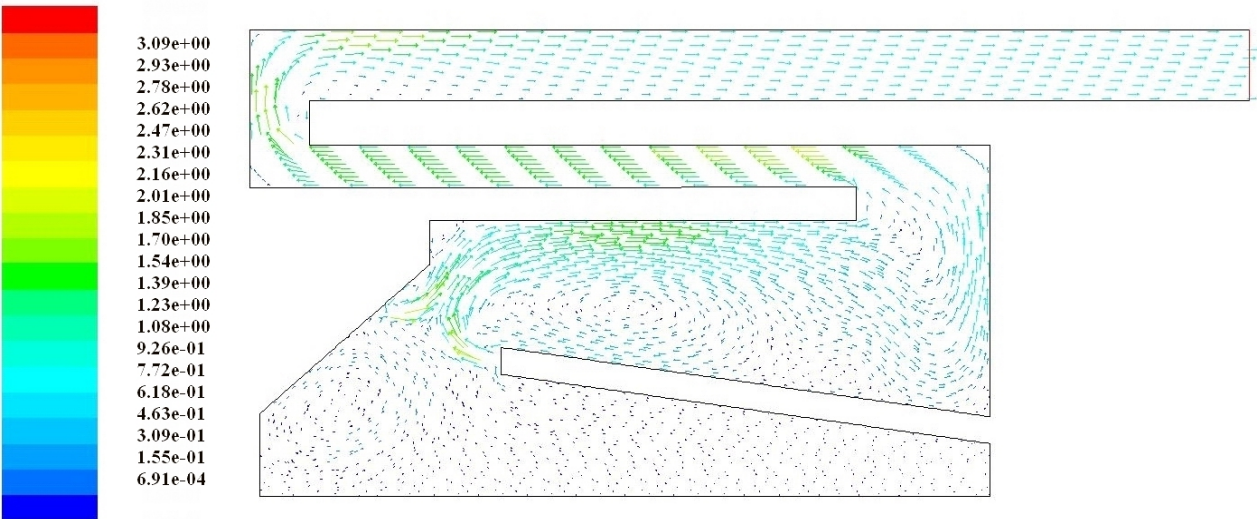
Velocity vectors colored by velocity magnitude (m/s)

(c) The rear arch coverage is 60 %, and the staged air distribution ratio is 4:6.

Velocity vectors colored by velocity magnitude (m/s)
(d) The rear arch coverage is 60 %, and the staged air distribution ratio is 2:8.

Velocity vectors colored by velocity magnitude (m/s)
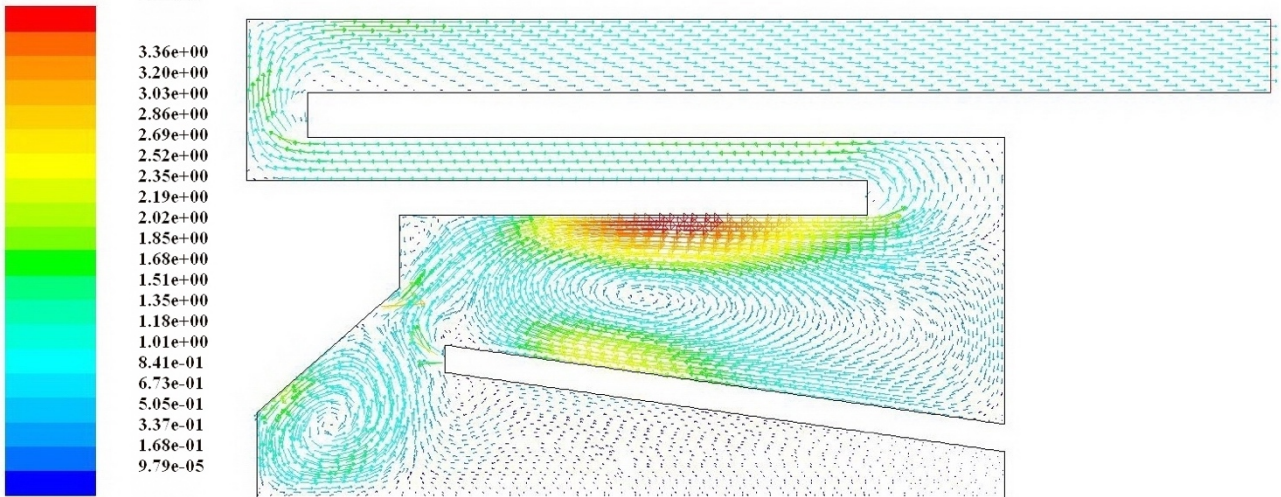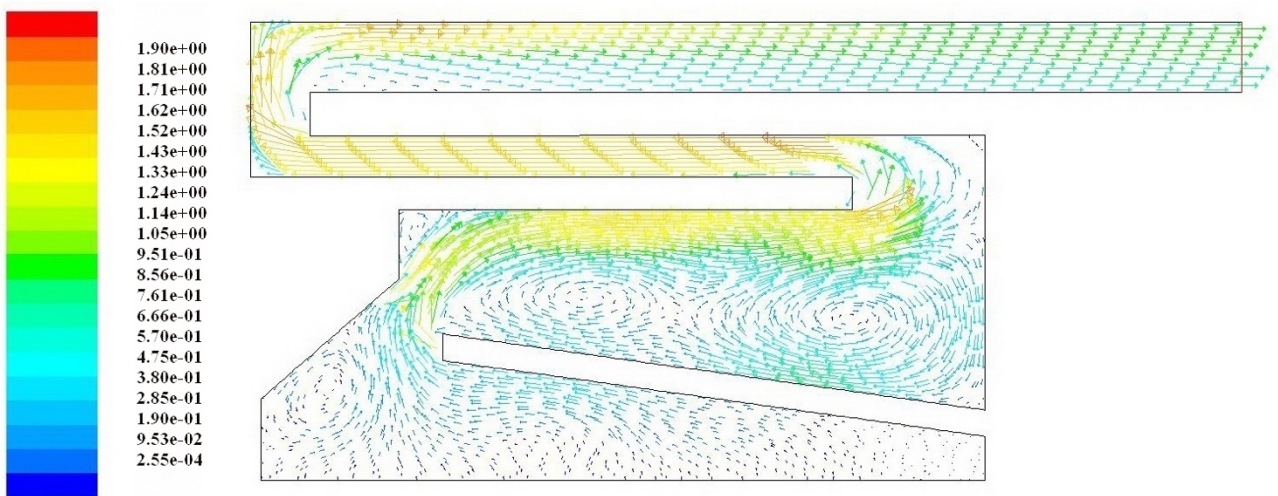(e) The rear arch coverage is 65 %, and the staged air distribution ratio is 4:6.

Velocity vectors colored by velocity magnitude (m/s)
(f) The rear arch coverage is 65 %, and the staged air distribution ratio is 6:4.
Fig. 3 Velocity vectors clouds in furnace under different rear arch coverage and staged air distribution ratios

(1) When the rear arch coverage is 55 %, α-shaped smoke flow cannot be formed effectively below the front and rear arches. With the increase in rear arch coverage to 65 %, an α-shaped eddy can be formed below the furnace

arch under all staged air distribution ratios, but the flow rates at the throat and secondary combustion space are excessively high to realize secondary combustion of smoke completely. With the increase in primary air, the eddy moves toward the front arch. When the rear arch coverage is 60 %, the best α-shaped eddy can be formed by adjusting the air distribution ratio, and the flow rate of flue gas in the secondary combustion space is inconsiderably fast.

(2) The formation of the α-shaped eddy motion is closely related to air distribution in addition to arch coverage. When the rear arch coverage is 60 % and 65 % and with the increase in primary air distribution, the α-shaped eddy shape becomes obvious but shrinks in size and moves toward the direction below the front arch.

(3) Secondary air influences the secondary combustion significantly. Under any rear arch coverage, a strong flue gas velocity can be formed above the rear arch in the secondary combustion zone regardless of the air distribution. Moreover, certain flame impingement against the furnace wall above the rear arch is observed. After the secondary air distribution ratio is decreased, the turbulence effect caused by secondary air declines, and the airflow decreases to laminar motion gradually. This phenomenon is relatively consistent with the downward trend of maximum airflow velocity when the rear arch coverage is 65 %. The residence time of smoke has to be increased to assure high-efficiency combustion of smoke in the secondary combustion space. Therefore, the secondary air distribution ratio can form an eddy in the secondary combustion space.

(4) Traditional coal-fired boilers generally have a long and high front arch at the maximum hot jet to assure successful ignition of fuels. A large front arch height is suggested to use due to the flammability and high volatility of biomass to prevent fast ignition of biomass.

To avoid the adverse impact of excess strength of the α-shaped eddy on combustion, the furnace structure is determined when the rear arch coverage is 60 % and the primary–secondary air distribution ratio is 4:6.

2.5 Selection for the heating surface of boiler and design of dust extraction system

Heat transfer in the boiler includes radiant and convective heat transfer. The radiant heat transfer surfaces include the water-cooled walls on the two sides below the gas pass of " 八 " shape, water walls on the two sides of the boiler, shell bottom, and smokestack outlet. The convective heat transfer surfaces mainly include the shell and transverse and longitudinal scouring surfaces of the gas pass. The size of the heating surface can be calculated in accordance with the thermodynamics of the furnace and tube bundle [34,35]. Relevant parameters are shown in Table 4. The dust extraction system is composed of a ceramic multicyclone dust collector and a pulse-jet fabric filter.

In sum, the furnace structure, grate size, and arch are calculated in accordance with the characteristics of fed fuels. The cold modeling experiment of the furnace shows that an α-shaped eddy can be formed below the arch when the rear arch coverage is 60 % and the staged air distribution ratio is

4:6, which minimizes the flame impingement phenomenon in the secondary combustion space.

3. Results and discussions

The experiment is performed in the duck hatchery and breeding area of Xinxiwang Liuhe Co., Ltd. in Feicheng County, Shandong Province. The performance test and fuel adaptability of boilers are accomplished in two steps. First, wood–straw mixed pellets (Φ8 mm), P. koraiensis pellets (Φ8 mm), and cotton straw briquette (32×32 mm) are chosen as main fuels for the boiler efficiency test on the basis of the local market of BMF. Second, the rice hull–duck manure briquettes (32×32 mm) and corn–wheat rods (Φ35 mm) produced by the factory are chosen to observe the combustion process. The fuel adaptability of the boilers is analyzed in accordance with the fuel properties. The rice hull–duck manure fuel, which has a high ash content, comes from the mixture of rice hull and duck manure paved on ground during the production of hatching eggs. The corn–wheat rods are mixed evenly at the ratio of 1:1. Industrial and element analyses of fuels are presented in Table 1.

3.1 Thermal performance test of boilers

The boiler efficiency test results when the three main fuels are used are shown in Table 5. The test results of the air pollutant emissions are shown in Table 6. The experimental results are summarized as follows:

(1) Biomass pellets have better combustion performance than briquettes. Table 5 indicates that the average heat output of a boiler is 715.76 kW/h, and the average boiler efficiency reaches 81.26 %. P. koraiensis pellets show the best fuel adaptability, followed by wood–straw mixed pellets and cotton straw briquettes. The positive balance efficiency of wood–straw mixed pellets is lower than that of cotton straw briquettes, but the boiler efficiency is higher. Even if the heat value of cotton straw is higher, the wood–straw mixed pellets still maintain good combustion performance. Briquettes with a larger volume than small particulate fuels have a smaller reaction surface area, thus causing slow flame front propagation, low combustion rate, and poor combustion stability. The experiment proves that particle size is an important influencing factor of combustion, and pellets show stronger combustion adaptability than briquettes.

(2) The boiler using BMF with a high ash content has low thermal efficiency. Boiler efficiency is negatively correlated with ash content. First, the heat value of the fuel is reduced by the nonflammable ash, which is mainly produced in the processes of harvest and transportation. Second, biomass fuel captures OH^- and H^+ in the combustion chain reaction during the formation of ash and inorganic salts (Si, Ca, Mg, etc.). The captured free radicals on the dust surface induce chemical inhibition of combustion. Lastly, silicate with a low-melting point is formed during combustion, which causes melted slag that is against combustion.

Table 5. Boiler efficiency test results

Items	Cotton straw briquettes	*P. koraiensis* pellets	Wood–straw mixed pellets
Circulation water flow G (kg/h)	16800	12360	29580
Feedwater temperature t_{js} (℃)	15	16.9	53.1

Drain water temperature t_{cs} (℃)	56.00	70.0	71.9
Fuel consumption B (kg/h)	200	186.00	186.00
Positive balance efficiency η_1 (%)	82.99	83.32	78.93
Heat loss due to unburned carbon in refuse q_4 (%)	10	0.26	2.76
Excess air ratio at smoke vent α_{py} (%)	1.73	2.16	1.67
Unburned combustible in slag C_{lz} (%)	26.5	11.28	18.8
Heat loss due to unburned gases q_3 (%)	0.06	0.07	0.42
Exhaust gas temperature t_{py} (%)	203.37	201.6	218.0
Heat loss due to exhaust gas q_2 (%)	11.06	14.18	13.50
Heat loss due to radiation q_5 (%)	1.80	1.63	1.82
Heat loss due to sensible heat in slag q_6 (%)	0.45	0.01	0.12
Sum of heat losses Σq (%)	26.90	16.14	18.63
Antibalance efficiency η_2 (%)	77.10	83.86	81.67
Boiler efficiency η (%)	80.05	83.59	80.15
Heat output Q (kW/h)	741.25	763.30	642.74

Table 6. Pollutant emission test results

Items	Cotton straw briquettes	*P. koraiensis* pellets	Wood–straw mixed pellets	Pollutant emission limit	
				GB13271-2014	The 13th Five-Year Plan for Biomass Energy
Dust concentration (mg/m^3)	7.9	5.6	8.8	50	20
SO_2 concentration (mg/m^3)	<5	<5	<5	300	50
NO_x concentration (mg/m^3)	1.9×10^2	1.0×10^2	1.6×10^2	300	200
Hg pollutant concentration (mg/m^3)	3.64×10^{-3}	1.12×10^{-2}	9.64×10^{-3}	0.05	—
Ringelmann emittance	<1	<1	<1	≤1	≤1

(3) Pollutant emissions are in compliance with the national standards of China, but NO_x emission is significantly influenced by N in fuels. Excessive nitrogen fertilizers are applied in the planting process of cotton, which lead to a high nitrogen content in cotton straw (Table 1). For the convenience of NO_x emission control by boiler operators, the relationship between exhaust gas temperature from the boiler of cotton straw briquettes (representing straw fuels with a high nitrogen content) and NO_x emission concentration (converted) is measured (Fig. 4). In fact, thermal NO_x emission increases when the excess air ratio is higher than 2.2, and NO_x emission concentration (converted) increases rapidly. Therefore, the exhaust gas temperature of a boiler fueled by biomass straw with a high nitrogen content is controlled within 210 °C to meet the more stricter emission standard of industrial heat boilers in the 13th Five-Year Plan for biomass energy.
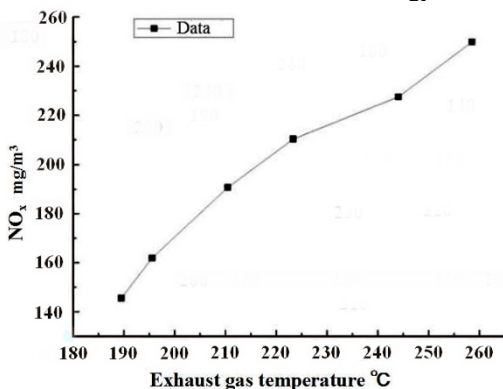

Fig. 4. Relationship between NO_x emission concentration from cotton straw briquette and exhaust gas temperature

3.2 Adaptability test of low-calorific-value fuels

After rice hull–duck manure briquettes enter into the boiler, the fuel layer upper surface keeps a small and low flame below the front arch. The fuel looks red from the position below the throat to the grate end, accompanied with the release of small blue flames in the fuel layer. The boiler heat output is less than 30 %. On the basis of the ash samples at the grate end, briquettes are burned completely, and the ash is similar to sandy soil after rubbing with hands. The corn–wheat rods show a basically consistent combustion state with rice hull briquettes, but the flame length below the front arch is slightly higher than that of the hull–duck manure briquettes. Local blue flames exist from the position below the throat to the front section of the grate under rear arch coverage. Incomplete combustion occurs in most internal structures of the fuel.

After the fuel enters below the front arch, the flame is relatively small, which is attributed to the high ash content and LHV. When the grate moves to the position below the throat, the airflow velocity is relatively high, while the furnace temperature is kept at a low level. The radiant and convective heat transfer between flue gas and the arches is inadequate to cause a vigorous combustion of the fuel layer. The blue flame on the fuel layer below the rear arch is caused by the combustion of high-concentration H_2, which is generated by fuels, and it is the sign of combustion of large particulate fuels. The sandy soil texture after briquette burning can be interpreted in two aspects. On the one hand, raw materials are molded into briquettes directly without dust removal. On the other hand, the SiO_2 content in rice

hull ash is relatively high [39], and silicates are formed after combustion due to the high temperature in the fuel bed. Tian [40] indicated that a higher ash content than 20 % is against the high-temperature combustion of BMF. Clearly, rice hull–duck manure fuel shall be upgraded. Although the ash content in corn–wheat rods is similar to that in cotton straw, the corn–wheat rods are still not burned completely, which might be related to the low calorific value and high content of alkali metals. As a result of the low calorific value of the fuel, combustion development toward the inner part is hindered when the alkaline-earth metals and minerals in ash form eutectic evaporate compounds [41].

Therefore, the combustion of low calorific BMF with large particle size, high ash content, and especially high contents of alkali metals is a sign of a loose fuel layer, a low burning rate, and slow heat release. The transient characteristics of combustion are generally evident, which are disadvantageous for combustion adjustment. Hence, fuel upgrading from the following two aspects is necessary.

(1) According to References [42,43], testing of ash and elements of design fuels is suggested to change the conversion potential of ash. Washing fuels with high ash content and low calorific value can eliminate ash effectively. Moreover, water-soluble Cl and S contents shall be decreased, and scorification and clustering of equipment shall be decelerated. Wood fuels can be added to increase the heat value if necessary.

(2) Decreasing the particle size of BMF and increasing the contact area between particles and air in the combustion process of the fuel layer are suggested to increase the heat release rate of flame.
The experimental results present that given equivalent heat value and ash content of design fuels, the boiler design goal can be realized when the rear arch coverage is 60 % and the staged air distribution ratio is 4:6. However, the adaptability of the biomass boiler to fuels with a low calorific value and large particles is poor, and fuel upgrading is needed.

4 Conclusions

The combustion performance and pollutant emission of a biomass boiler are mainly determined through furnace, arch, and air staging. This study designs a 1 t/h biomass chain boiler and conducts a cold modeling experiment on the flue gas in the furnace on the basis of Ansys-Fluent software. Moreover, a thermal performance test of the biomass boiler is performed. The major conclusions are drawn as follows:

(1) When the rear arch coverage and staged air distribution ratio are 60 % and 4:6, respectively, flue gas can form an "α-shaped" flow below the arch, which prolongs the residence time of smoke and decreases the flame impingement phenomenon in the secondary combustion space as much as possible. Combustion performance tests of main and auxiliary fuels in the market are implemented. The boiler efficiency of all main fuels is higher than 80 %, with the Ringelmann emittance and the pollutant, SO_2, and Hg emission concentrations all meeting standards.

(2) The thermal NO_x emission of fuels is increased when the excess air ratio is higher than 2.2. The excess air ratio shall be controlled to lower than 2.1 and the exhaust smoke temperature shall be controlled within 210 °C for high-nitrogen straw particles to meet the more stricter NO_x emission standards in 13th Five-Year Plan for biomass energy of the People's Republic of China.

(3) Fuel particle size and ash content can influence boiler operation significantly. With the increase in particle size and ash content, the heat release rate slows down gradually, accompanied with increasing difficulties in boiler firing adjustment and a sharp reduction in thermal efficiency. The biomass boiler is fueled using pellets and briquettes with LHV between 3200 and 4200 kcal/kg, and it shall be examined if necessary to assure a small fluctuation in fuel mass. High-ash-content fuels are suggested to be washed directly to eliminate ashes and increase heat value. The particle size of BMF shall also be decreased to increase the contact area between the fuel layer and air and the combustion efficiency.

This study provides references to the arch design and air staging of a 1 t/h biomass boiler. In future studies, the secondary air distribution ratio shall be further optimized to improve the reasonability of flue gas, promote the combustion performance further, and lower the pollution emission. This study is of high significance to the design of small-scale industrial heating boilers.

References

1. Paredes-Sánchez, J. P., López-Ochoa, L. M., López-González, L. M., las-Heras-Casas, J., Xiberta-Bernat, J., "Energy utilization for distributed thermal production in rural areas: A case study of a self-sustaining system in Spain". *Energy Conversion and Management*, 174, 2018, pp. 1014-1023.
2. Soltero, V. M., Chacartegui, R., Ortiz, C., Velazquez, R., "Potential of biomass district heating systems in rural areas". *Energy*, 156, 2018, pp. 132-143.
3. Cong, H. B.,Yao, Z. L., Zhao, L. X., Meng, H. B., Huo, L. L., Yuan Y. W., Ren, Y. W., Liu, G. H., Liu, S. Y., "Technical and economic evaluation for clean heating using straw in rural area based on principle of value engineering". *Transactions of the Chinese Society of Agricultural Engineering*, 35(9), 2019, pp. 200-205. (in Chinese)
4. Tian, Y. S., "Research on the development path of deeply coupling utilization of coal and new energy". *Energy of China*, 42(5), 2020, pp. 25-30. (in Chinese)
5. Sun, L. N., Ma, X. Y., Liu, K. B., Zheng, X. H., Zhang, H. L., Rong, L. G., "A review on research advances on microbial treatment and strengthening techniques of crop straw". *Journal of Shenyang University* (*Natural Science*), 30(3), 2018, pp. 188-195.
6. He, G. J., Liu, T., Zhou, G., "Straw burning, PM2.5, and death: evidence from China". *Journal of Development Economics*, 145, 2020, pp. 102468
7. Seglah, P. A., Wang, Y. J., Wang, H. Y., Bi, Y. Y., Zhou, K., Wang, Y., Wang, H., Feng, X. X., "Crop straw utilization and field burning in northern region of Ghana". *Journal of Cleaner Production*, 261, 2020, pp. 121191.

8. Su, J. L., Luo, X. J., Jiao, Z. W., Huang, H. Z., "Combustion and emission characteristics of boiler using pelletized biomass fuel". *Journal of Jilin University* (*Engineering and Technology Edition*), 40(4), 2010, pp. 953-958.

9. Prasad, S., Singh, A., Korres, N. E., Rathore, D., Sevda, S., Pant, D., "Sustainable utilization of crop residues for energy generation: a life cycle assessment (LCA) perspective". *Bioresource Technology*, 303, 2020, pp. 122964

10. Jiang, L., Xue, B., Ma, Z. X., Yu, L., Huang, B. J., Chen, X. P., "A life-cycle based co-benefits analysis of biomass pellet production in China". *Renewable Energy*, 154, 2020, pp. 445-452

11. Xu, J., Liu, S. N., Jiang, Y., Yuan, Z. H., "Policy analysis and implementation of biomass molding fuels industry in China". *Advances in New and Renewable Energy*, 3(6), 2015, pp. 477–484 (in Chinese).

12. Suryaningsih, S., Nurhilal, O., Yuliah, Y., Mulyana, C., "Combustion quality analysis of briquettes from variety of agricultural waste as source of alternative fuels". In: *International Conference on Biomass: Technology, Application, and Sustainable Development, 2016*, Bogor, Indonesia: IOP Publishing Ltd., 2017, pp. 012012.

13. Buchmayr, M., Gruber, J., Hargassner, M., Hochenauer, C., "Experimental investigation of the primary combustion zone during staged combustion of wood-chips in a commercial small-scale boiler". *Biomass and Bioenergy*, 81, 2015, pp. 356-363.

14. Fournel, S., Palacios, J. H., Morissette, R., Villeneuve, J., Gdobout, S., Heitz, M., Savoie, P., "Influence of biomass properties on technical and environmental performance of a multi-fuel boiler during on-farm combustion of energy crops". *Applied Energy*, 141, 2015, pp. 247-259.

15. Ko, S., Lautalal P., "Optimal level of woody biomass co-firing with coal power plant considering advanced feedstock logistics system". *Agriculture*, 8(6), 2018, pp. 74.

16. Pawlak-kruczek, H., Arora, A., Mościcki, K., Krochmalny, K., Sharma, S., Niedzwiecki, L., "A transition of a domestic boiler from coal to biomass-Emissions from combustion of raw and torrefied Palm Kernel shells (PKS)". *Fuel*, 263, 2020, pp. 116718.

17. Niu, Y. Q., Lv, Y., Lei, Y., Liu, S. Q., Liang, Y., Wang, D. H., Hui, S. E., "Biomass torrefaction:properties, applications, challenges, and ecomomy". *Renewable and Sustainable Energy Reviews*, 115, 2019, pp. 109395.

18. Loo, S. V., Koppejan, J., "*Handbook of Biomass Combustion and Co-firing*". London: Earthscan, UK, 2007. pp.52-86.

19. Chu, J. F., "*Numerical simulation study on influence of arch and air distribution mode for combustion performance in reciprocating furance*". Master thesis of Harbin Institute of Technology, China, 2014, pp. 18-45.

20. Just, W., Ciupek, B., Urbaniak, R., "Numerical study of heat transfer process in a low power heating boiler equipped with after burning chamber". *Energy*, 196(1), 2020, pp. 117093.

21. Zhai, W. L., Liu, S. Y., Guan, Z. Y., Wang, P. X., Liu, H. F., Xia, X. N., Tang, Y. T., "Development of chain-steam boiler for biomass briquette". *Transactions of the Chinese Society of Agricultural Engineering*, 32(1), 2016, pp. 243－249. (in Chinese)

22. Guo, F. Q., Dong, Y. P., Dong, L., Jing, Y. Z., Yan, Y. X., "Design and low NOx emission effect of biomass briquette boiler with third air distribution type". *Transactions of the Chinese Society of Agricultural Engineering*, 28(14), 2012, pp. 42－46. (in Chinese)

23. Sun, K., Chen, C., Xu, Y., Liu, Y., Zhu, G. Z., Ying, H., "Design and experiments study on combustion engine of straw briquettes fuel". *Chemistry and Industry of Forest Products*, 34(6), 2014, pp. 93-99.(in Chinese).

24. Pei, J. J., Wang, H. M., You, C. F., "Optimization of staged combustion in a 600 MWe tangentially fired boiler with wall air injection". *Fuel*, 275, 2020, pp. 117951.

25. Wang, W. S., Huang, Z. H., Tian, M., Wang, J. H., Shangguan, S. S., Yao, M. Y., "Numerical simulation of NOx emission characteristics during combustion in 350MW supercritical cogeneration tangentially boiler". *Thermal Science*, 24(5A), 2020, pp. 2717-2728.

26. Zhou, A. Q., Tu, Y. J., Xu, H. P., Yang, W. M., Zhao, F. Y., Boon, S. K., Subbaiah, P., "Numerical investigation the effect of air supply on the biomass combustion in the grate boiler". *Energy Procedia*, 158, 2019, pp. 272-277.

27. Song, G. L., "*Boiler Calculation manual*". Shenyang: Liaoning Science and Technology Publishing House, China, 1995, pp. 910-913.

28. Zheng, K. X., "*Design and study on furnace and grate of 4t/h biomass briquette mechanical boiler*". Master thesis of Henan Agricultural University, 2013, pp. 19-20. (in Chinese)

29. Chse, J. S., Zhang, M. Y., Yang, S. J., Rho, H. J., Lee, J. W., Ohm, T. I., "A study on the secondary air injection method of the combustor considering characteristics of solid fuels". *Waste and Biomass Valorization*, 11(8), 2020, pp. 4535–4550.

30. Song, M. H., Zeng, L. Y., Chen, Z. C., Li, Z. Q., Kuang, M., "Aerodynamic characteristics of a 350-MWe supercritical utility boiler with multi-injection and multi-staging: Effects of the inner and outer secondary air distribution in the burner". *Journal of the Energy Institute*, 91(1), 2018, pp. 65-74.

31. Luo, Y. H., Zhang, M., Deng, R. Q., Cao, Y., "Study of the low NOx combustion technology for biomass-fired grate boilers". *Journal of Chinese Society of Power Engineering*, 38(12), 2018, pp. 957-964. (in Chinese)

32. Chen, R., Yue, H. H., Yue, R., Ai, Y., Zheng, J. X., "Numerical simulation of combustion in a biomass briquette chain boiler". *Biomass Conversion and Biorefinery*, 2020, doi: 10.1007/s13399-019-00569-0.

33. Chen, R., Rao, Y., Yue, H. H., Ai, Y., Zhang, X., Zhang, L. L., Zheng, J. X., "Numerical simulation of bed combustion in biomass-briquette boiler". *Journal of Energy Engineering*, 146(4), 2020, pp. 04020031.

34. Le, J. M., Ye, W. H., Cheng, L. M., Huan, B. W., Yang, L. D., "*Methods of Calculation and design for industrial boiler*" . Beijing: Standards Press of China, China, 2005, pp. 33-46.

35. Li, Z. G., Liang, Y. D., Niu, Q. Z., "*Modern design and development of industrial boilers*". Beijing: Standards Press of China, China, 2011, pp. 1-16.

36. Fu, C. G., Hou, S. L., Tian, Y. S., Zhao, L. X., Meng, H. B., "Analysis of the influence factors of biomass layer combustion process". *Renewable Energy Resources*. 31(10), 2013, pp. 120-125. (in Chinese)

37. Gaze, B., Noszczyk, T., Romanski. L., Dyjakon, A., Kulazynski, M., "Determination of the dominant mechanism for NOx formation in low power boilers fed with biomass". *Przemysl Chemiczny*, 99(2), 2020, pp. 228-233.

38. Ji, J. J., "*Numerical modelliing of the combustion in coal-fired travelling grate boilers and the optimzation of arch and air distribution*". Doctoral Dissertation of Shanghai Jiao Tong University, China, 2008, pp.23-49.

39. Akter, S., Rahaman, Md. D., Khan, M. N. I., Hossain, A. K. M. A., "Synthesis, structural, morphological, electrical and magnetic properties of (1-x) [Ni$_{0.35}$Cu$_{0.15}$Zn$_{0.50}$Mn$_{0.05}$Fe$_{1.95}$O$_4$] +(x) [rice husk ash] composites". *Materials Research Bulltin*, 112, 2019, pp. 182-189.

40. Wang, Y. Q., Tian, Y. S., Hou, S. L., Zhao, L. X., Meng, H. B., "Experiment on fuel flexibility of biomass pellet burner". *Transactions of the Chinese Society of Agricultural Engineering*, 30(7), 2014, pp. 197－205. (in Chinese)

41. Meng, X. X., Sun, R., Ismail, T. M., Zhou, W., Ren, X. H., Zhang, R. H., "Parametric studies on corn straw combustion characteristics in a fixed bed :Ash and moisture content". *Energy*, 158, 2018, pp. 192-203.

42. Rebbling, A., Sundberg, P., FagerstrÖm, J., Carborg, M., Tullin, C., Bostrom, D., Ohman, M. Boman, C., Skoglund, N., "Demonstrating fuel design to reduce particulate emission and control slagging in industrial-scale grate combustion of woody biomass". *Energy Fuels*, 34(2), 2020, pp. 2574–2583.

43. Fu, C. G., Tian, Y. S., Li, S. Z., Hou, S. L., Zhao, L. X., Meng, H. B., "Experimental study of fuel performance improvement on fermented residue of sweet sorghum stalk by water-washing pretreatment". *Acta Energiae Solaris Sinica*, 38(1), 2017, pp. 78-84. (in Chinese)